Vol.10, Issue No 3, Sep 2020

FLOW-BOILING OF R134A REFRIGERANT HOW THE MICROFIN TUBE AFFECTS HEAT TRANSFER

Dr.Naveen.R,S.K.Sharanabasappa,Rajesh.J

Asst. Prof,Assoc. Prof,Asst. Prof

shivaganesh.ng@gmail.com, Sk_hpt@yahoo.com, rajeshjavali@gmail.com

Department of Mech, Proudhadevaraya Institute of Technology, Abheraj Baldota Rd, Indiranagar, Hosapete, Karnataka-583225

Abstract:
The impact of flow boiling on the longevity and effectiveness of HVAC systems is the primary focus of this study. This study aims to examine the properties of the heat transmission of the refrigerant R134a in two types of tubes: smooth and microfin. The outside diameter of the tubes is 9.52 mm. Microfin tubes have 1.62 times more surface area than smooth tubes due to their unique shape with a 46° apex angle and a 22° helix angle. This work uses an extensive experimental analysis to look at how four important characteristics affect heat transfer coefficients: mass flux, saturation temperature, heat flux, and average vapour quality. Specifically, at a mass flux of G = 125 kg m⁻2•s·⁚·1, the HTC shows significant improvements, although it faces problems with dry-out at high vapour quality levels. Regardless of the operating circumstances, the findings show that microfin tubes have heat transfer coefficients that are up to 270% greater than smooth tubes. Computational research using genuine flow boiling heat transfer models further validates the experimental findings, showing a high degree of concordance.

1. Introduction

Heating, ventilation, and air conditioning (HVAC) systems exhibit a salient function in various applications by providing indoor assistance, controlling temperature and humidity levels, and maintaining air quality. HVAC systems are significant energy consumers, especially in commercial and industrial settings. The energy sources used to power HVAC systems, such as natural gas or coal-generated electricity, have the potential to emit greenhouse gases, namely, carbon dioxide (CO_2) and methane (CH_4). HVAC systems utilize refrigerants to facilitate the heat transfer process. Several refrigerants from previous generations, specifically chlorofluorocarbons (CFCs) and hydrochlorofluorocarbons (HCFCs), have properties that cause the ozone layer to deplete (known as ozone depletion potential, ODP) and worsen global warming (known as global warming potential, GWP). Research and development on flow boiling exhibit a salient function in the ongoing improvement of HVAC systems, focusing on boosting their efficiency and environmental sustainability [1–3]. Selecting a refrigerant for an HVAC system is a critical decision influenced by various factors, including environmental considerations, performance requirements, safety concerns, and compliance with regulatory standards.

Consequently, ongoing endeavors are underway to improve the advancement of refrigerants and produce compounds that are even more ecologically viable and have reduced global warming potentials. Researchers are driven to examine the effects of choosing pure or mixed refrigerants with different factors, such as heat transfer, overall system performance, as well as environmental consequences. The decision to improve the inner tube of an evaporator is a purposeful strategic action aimed at achieving improved energy efficiency, cost reduction, and higher system per- formance. These enhancements greatly enhance HVAC systems' efficiency and long-term sustainability in various settings. Microfin tubes are increasingly chosen as a pre- ferred option for internal alterations in unitary equipment due to their combination of improved heat transfer, small size, energy economy, adaptability, cost-effectiveness, and enhanced refrigerant performance. Microfin tubes are effi- cient, space-saving, and cost-effective solutions in the design and manufacturing of evaporators [4, 5]. This involves the analysis of several factors, including heat transfer coefficients (HTCs) and the influence of different operational conditions [6–14].

Current research has mostly focused on microfin tubes, examining the effectiveness of different refrigerants in both microfinned and smooth tubes. Hambraeus et al. [15] conducted a test for examining HTCs of R134a. Their investigation employed ten test sections arranged linearly. Notably, at the lowest heat flux (q) of 3.2 kW m^{-2}, the HTC remained relatively stable until a vapor quality (x) of 0.90 was exceeded, after which a decline was observed. Kedzierski et al. [16] compared HTC and bubble formation for different refrigerants, including R134a, during boiling at a vapor quality of approximately 0.01. Their findings highlighted R134a′s superior heat transfer efficiency compared to R12, primarily attributed to a 38% higher bubble production rate. Interestingly, these results diverged from earlier studies, emphasizing the significant role of enriched heat transfer in the liquid phase for R134a, as opposed to R12. Meanwhile, Huo et al. [17] elucidated flow evaporation in tubes with diameters of 4.26 and 2.01 mm, utilizing R134a refrigerant and also systematically varied test parameters, including mass flux (G) ranging from 101 to 501 $kg{\cdot}m^{-2}{\cdot}s^{-1}$, pressure from 8 to 12 bar, vapor quality up to 0.85, and heat flux from 13 to 150 $kW{\cdot}m^{-2}$. Their findings indicated nucleate boiling predominated when the vapor quality was below approximately 0.40–0.50 for the 4.26 mm tube and 0.20–0.30 for the 2.01 mm tube. In addition, Bandarra Filho et al. [18] conducted a study on boiling (specifically convective boiling) using six test sections employing R134a refrigerant. The outer diameters (ODs) ranged from 6 to 9.52 mm. Despite some uncertainty in the experimental parameters (including G values and x values), the authors utilized Martinelli's correlations to analyze the impact of friction on flow patterns. Their proposed correlation focused on interpreting experimental data related to annular and misty flow patterns. The study conducted by Greco et al. [19] examined several factors that influence convective boiling heat transfer. They analyzed how G and q affected the HTC. The researchers discovered a direct relationship between the G, high q, and HTC. Furthermore, they noted that a modification in vapor quality impacted the HTC. The void fraction of smooth as well as grooved tubes using R134a in a horizontal test setup was investigated by Koyama et al. [20]. Experimental conditions for the smooth tube included a length (L) of 1.024 m, G ranged from 125 to 250 $kg{\cdot}m^{-2}{\cdot}s^{-1}$, OD of 9.53 mm, and ID of 7.51 mm. Similarly, microfin tube had L of 1.015 m, G ranged from 90 to 180 $kg{\cdot}m^{-2}{\cdot}s^{-1}$, OD of 9.53 mm, and ID of 8.87 mm. Operating situation covered ranges from x � 0.01 to 0.96, with corresponding saturation pressure (P_{sat}) values of 1.2−0.8 MPa. The study examined void fraction within both smooth and grooved tubes, concluding that a pressure loss resulted in an enrichment in the void fraction, with the microfinned tube having a greater impact on the void fraction.

Cui et al. [21] examined characteristics of R134a flowing within a microfin tube. The study maintained an evaporative pressure of 500 kPa, varying G from 61 to 315 $kg{\cdot}m^{-2}{\cdot}s^{-1}$ and q from 3 to 21.8 $kW{\cdot}m^{-2}$. The researchers observed distinct flow regimes at different microfin levels, with stratified flow predominantly at low G. Hatamipour et al. [22] conducted a study to investigate flow boiling of smooth and microfin tubes with R134a. They aimed to identify flow regimes and heat transfer characteristics. Experimental conditions were varied, including saturation temperature (T_{sat}), mass flux, heat flux, and vapor quality. Annular flow occurred at higher vapor quality, while stratified-wavy flow occurred at lower vapor quality. Researchers observed that HTC for microfin tubes has been 6% higher in comparison with smooth tubes under similar mass flow conditions. Colombo et al. [23] delved into the behavior of refrigerant R134a in horizontal microfin tube, focusing on evaporation characteristics. Experimental conditions involved a T_{sat} of 5°C, G ranging from 100 to 340 $kg{\cdot}m^{-2}{\cdot}s^{-1}$, q values between 3.2 and 17.8 $kW{\cdot}m^{-2}$, vapor quality from 25% to 70%, and an OD of 9.52 mm. Findings confirmed that HTC was enriched with lower mass flux during evaporation and heat flux notably influenced HTC. Similarly, Abadi et al. [24] performed experimental studies using R245fa and R134a in vertically oriented tube with specific dimensions.

In their comprehensive study, Wen et al. [25] docu- mented the heat transfer properties of R134a refrigerant as it flowed through an aluminum microchannel. The researchers noted that the HTC enriched in amplitude as the diameter of the microchannel was widened. The research conducted by Diani et al. [26–28] investigated the phenomenon of forced convective heat transfer using horizontal micro-fin conduit with ID of 3 mm. The researchers observed microfinned tubes demonstrated superior HTC when subjected to low vapor quality and high q values compared to flat tubes. A positive association between HTC and vapor quality was observed. In addition, Celen et al. [29] observed that the average HTC of R134a increases as T_{sat} increases in flow boiling heat transfer setting. This observation had been consistent in both conventional and modified tubes. When comparing microfin tubes to flat tubes, HTC of microfin tubes has been significantly high, showing an improvement of 1.9 times. Righetti et al. [30] examined the behavior of R1233zd(E) in grooved tube having ID of 4.3 mm;

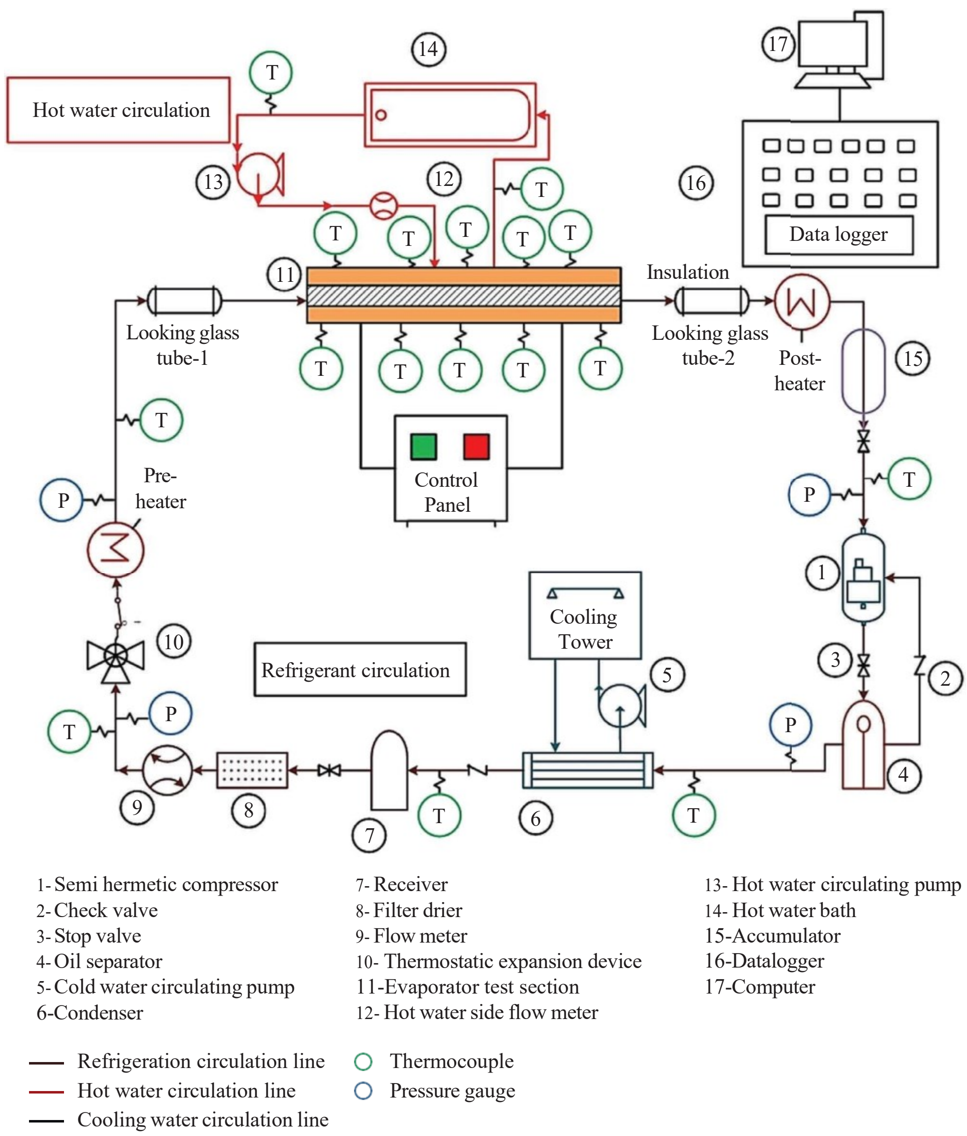

FIGURE 1: Illustration depicting the setup of the experimental test equipment.

TABLE 1: Thermophysical characteristics of the refrigerant [35].

Refrigerant						R134a	
ODP						0	
GWP						1430	
M, (kg·kmol^{-1})						102.03	
ASHRAE safety guide						A1	
Composition						Pure	
T_{crit}, (K)						347.25	
P_{crit}, (kPa)						4059.28	
T_{sat} (K)	P_{sat} kPa	ρ_l (kg·m^{-3})	μ_l (μPa·s^{-1})	i_{lv} (kJ·kg^{-1})	k_l (kW·m^{-1}·K^{-1})	$C_{p,l}$ (kJ·kg^{-1}·K^{-1})	σ (mN·m^{-1})
290.15	520.52	1236.2	215.24	184.89	84.579	1.3939	9.1657
295.15	607.89	1218.0	202.28	180.51	82.423	1.4125	8.4841

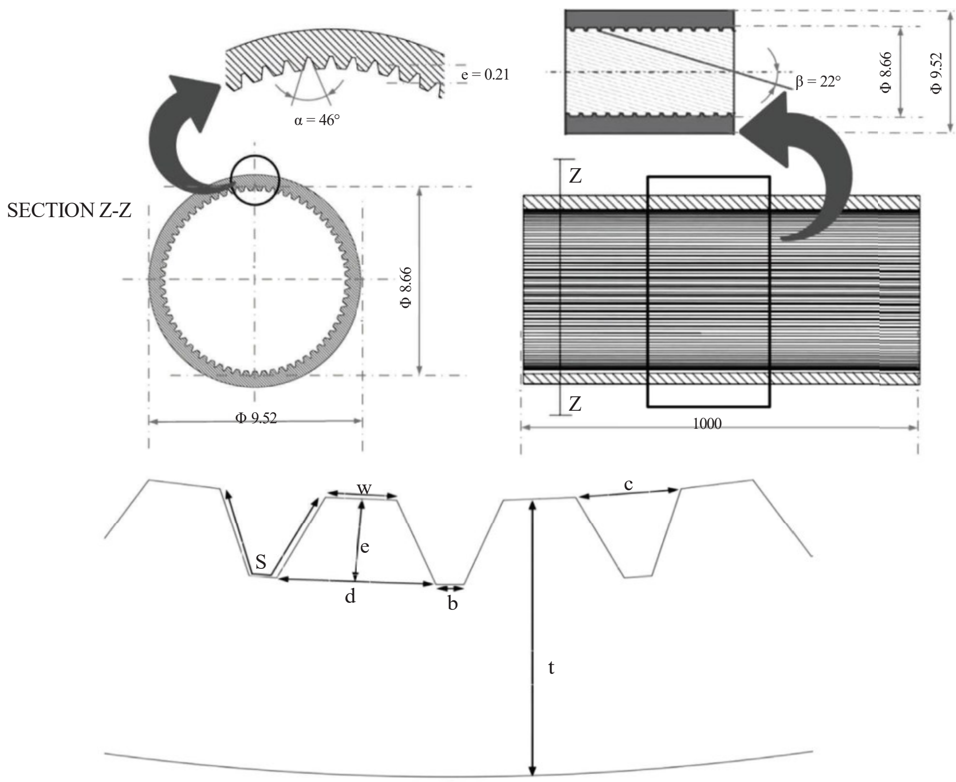

FIGURE 2: Details of the micro-fin test tube.

TABLE 2: Testing tube geometries.

Geometrical variable	Unit	Smooth tube	Microfin tube
OD	mm	9.52	9.52
ID	mm	8.66	8.66
t	mm	0.43	0.43
e	mm		0.21
S	mm		0.6279
b	mm		0.1785
c	mm		0.3272
d	mm		0.2749
w	mm		0.1042
β	(°)		22
α	(°)		46
N_{fin}			60
L	mm	1000	1000
A_c	mm^2	58.9014	56.5131
A_s	mm^2	27206	43926

TABLE 3: Testing conditions.

Refrigerant	G (kg·m^{-2}·s^{-1})	T_{sat} (K)	x_{avg}	q (kW·m^{-2})
R134a	75, 125, 175	290.15, 295.15	0.02–0.9	12, 18, 24

a lessening in thermal conductivity was observed, mostly associated with the phase transition event. However, HTC consistently improved regardless of the G value, even when exposed to low q values below 30 kW m^{-2}.

10 to 80 kW m^{-2} and maintaining continuous heat flux of 60 kW m^{-2} on hot water side. This study showed significant improvement in the HTC. However, using a microfin tube led to vapor quality up to 0.5, where initially, the HTC improved but then declined as vapor quality increased.

Further tests were done by Deb et al. [32] to investigate boiling behavior of R407c within both horizontal smooth and microfin tubes. Test conditions included T_{sat} of 283.15 K and 303.15 K and heat flux ranged from 5 to 80 kW m^{-2}. Notably, the micro-fin tube exhibited significantly higher HTC compared to the smooth tube, with enhancements ranging from 28% to 280%. In addition, Vidhyarthi et al. [33] explored the effects of various materials on an evaporator during flow boiling of refrigerant R134a. Their study maintained a constant T_{sat} of 10°C, with G ranging from 101 to 301 kg m^{-2}·s^{-1} and q from 20 to 60 kW m^{-2}. Among the selected tubes, copper tubes with vapor quality up to 0.8 exhibited the highest HTC. Furthermore, Deb et al. [34] documented the heat transfer performance of R22 and R407c in micro-fin tube. They varied G from 151 to 351 kg m^{-2}·s^{-1}, q from 20 to 80 kW m^{-2}, and maintaining T_{sat} of 293 and 313 K. The test data aligned well with established correlations for microfin tubes, with 85% and 95% falling within error margins of ±15% and ±30%, respectively. Interestingly, the study revealed that R22 exhibited a higher HTC than R407c.

The current study focused on performing experimental research to examine heat transfer properties of R134a re- frigerant within both a smooth tube and a microfin tube. The research introduces a unique feature of a testing tube with a specific microfin structure, characterized by different helix and apex angle as 22° of 46°, respectively. Our research focused on the impact of various parameters, including G, q, T_{sat}, and average vapor quality (x_{avg}), on the HTC. To assess the precision of our investigations, we compared our experimental results with established flow boiling correlations.

2. Experimental Approach

The primary constituents of the configuration are disclosed in Figure 1. The testing tube has been heated using liquid (water) heating. The comprehensive experimental methodology is outlined in Vidhyarthi et al. [33]. An assessment is conducted to establish the characteristics of flow boiling, namely, the parameters G, q, T_{sat}, and x_{avg}, for R134a. Table 1 exhibits a comprehensive overview of the properties of the R134a refrigerant. Multiple parameters were considered when determining the test tube and microfin tube dimensions. These criteria included the tube's length, helix angle, apex angle, fin height, ID, and OD. The microfin tube has OD of 9.52 mm and ID of 8.66 mm, as shown in Figure 2. Table 2 presents comprehensive technical specifications of the improved evaporator testing module. Table 3 displays the spectrum of input parameters used during the testing process.

The refrigerant circulation system includes several critical components: water-cooled condenser, oil separator, filter drier, receiver, a semihermetic compressor, flow meter, thermostatic expansion valve, pre- and postheaters, and an evaporator test section. The condenser, designed with a water-cooled counterflow shell-and-tube arrangement, connects to compressor. The refrigerant undergoes a phase shift in the condenser shell, transforming into a low- pressure, high-temperature liquid. Water, cooled in a tower, flows through the condenser tubes. A receiver stores the liquid refrigerant, which then passes through a dryer before reaching to expansion valve. Furthermore, refrigerant proceeds through preheater and enters in flow meter for accurate mass flow rate measurement. An electric heater maintains water temperature in a recirculating system, regulated by a thyristor regulator. The system employs a shell-and-tube heat exchanger having counterflow con- figuration. Finally, the postheater ensures complete vapor- ization of the liquid refrigerant before it accumulates and returns to the compressor. T-type and K-type thermocou- ples monitor fluid temperatures at various points.

Table 4: Uncertainty involved in the experiment.

	Uncertainty
Quantitative variables	
L	±0.1 mm
D	±0.1 mm
T	±0.1°C
$\dot{m}_{ref}$	±1%
$\dot{m}_w$	±1%
Estimated variables	
Vapor quality	1.02–5.57%
q	2.79%
HTC	4.6–14.85%

3. Data Reduction

Heat transfer rates are balanced by the refrigerant and the water, which can be written as follows [29]:

$$Q_w = Q_{ref,ts} = \dot{m}_w \times C_{p,w} \times \left(T_{w,ts,out} - T_{w,ts,in}\right). \tag{1}$$

The enthalpy of the refrigerant at the intake of the tube is as follows:

$$i_{ref,in} = \frac{i_{ref,ph,l,in} + Q_{ph,latent}}{\dot{m}_{ref}}. \tag{2}$$

Here,

$$Q_{ph} = Q_{ph,sens} + Q_{ph,latent}, \tag{3}$$

$$Q_{ph,sens} = \dot{m}_{ref} \times C_{p,l,ref} \times \left(T_{ref,ph,out} - T_{ref,ph,in}\right). \tag{4}$$

Similarly, the quantity of heat absorbed by the refrigerant can be transferred to the outlet enthalpy of the refrigerant as follows:

$$i_{ref,out} = \frac{i_{ref,in} + Q_{ref,ts,latent}}{\dot{m}_{ref}}, \tag{5}$$

$$Q_{ref,ts,sens} = \dot{m}_{ref} \times C_{p,l,ref} \times \left(T_{ref,ts,out} - T_{ref,ts,in}\right), \tag{6}$$

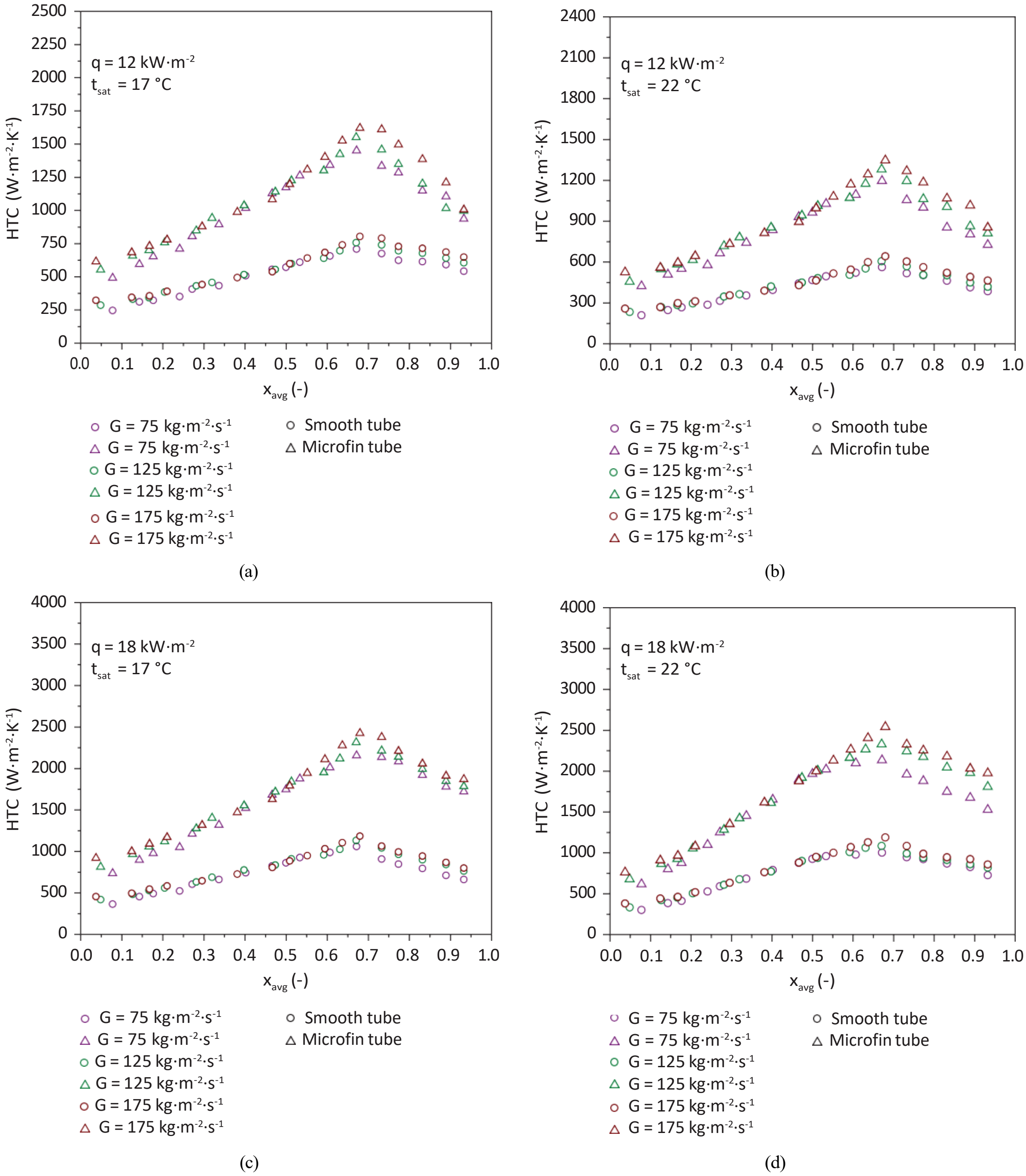

FIGURE 3: Continued.

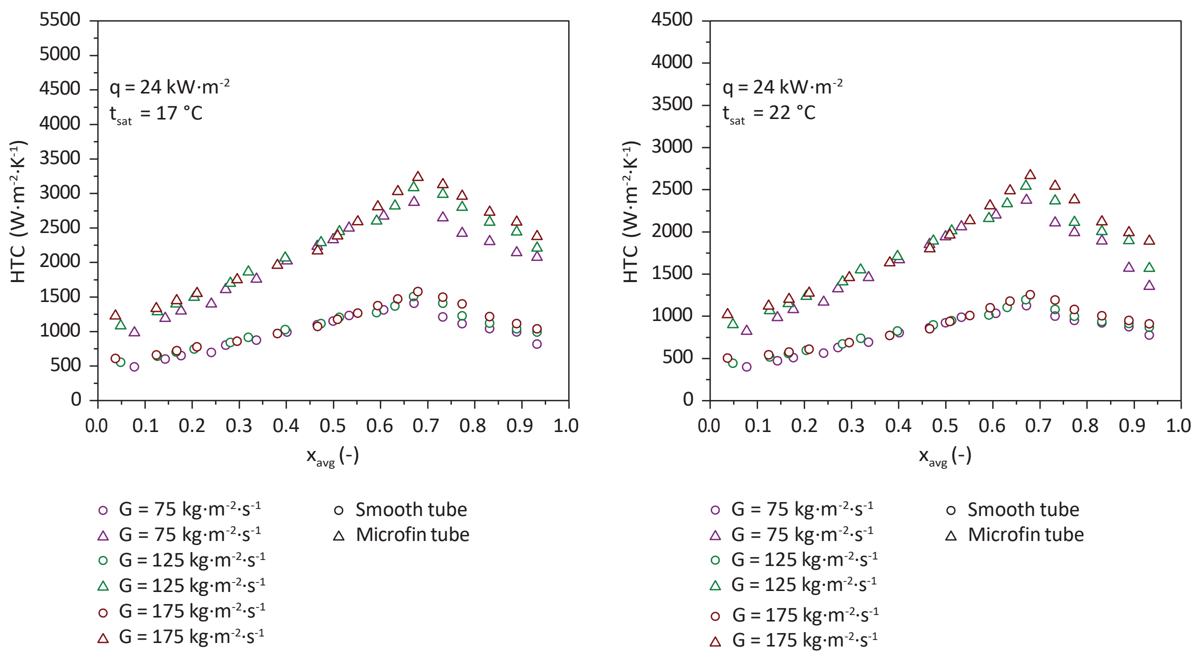

(e) (f)

FIGURE 3: Influence of mass flux on HTC. (a) $t_{sat} = 17$°C, $q = 12\,\mathrm{kW{\cdot}m^{-2}}$, (b) $t_{sat} = 22$°C, $q = 12\,\mathrm{kW{\cdot}m^{-2}}$, (c) $t_{sat} = 17$°C, $q = 18\,\mathrm{kW{\cdot}m^{-2}}$, (d) $t_{sat} = 22$°C, $q = 18\,\mathrm{kW{\cdot}m^{-2}}$, (e) $t_{sat} = 17$°C, $q = 24\,\mathrm{kW{\cdot}m^{-2}}$, and (f) $t_{sat} = 22$°C, $q = 24\,\mathrm{kW{\cdot}m^{-2}}$.

$$Q_{ref,ts,latent} = Q_{ref,ts} - Q_{ref,ts,sens}. \tag{7}$$

Also, the inlet and outlet vapor quality (x) are given as follows:

$$x_{in} = \frac{i_{ref,in} - i_{ref,l,in}}{i_{ref,lv,in}}, \tag{8}$$

$$x_{out} = \frac{i_{ref,out} - i_{ref,l,out}}{i_{ref,lv,out}}. \tag{9}$$

x_{avg} is given as follows:

$$x_{avg} = \frac{(x_{in} + x_{out})}{2}. \tag{10}$$

The equation used to compute the two-phase HTC of the refrigerant is presented in the following:

$$h_{tp} = \frac{Q_{ref,ts,sens}}{A_{in} \times (T_{sat} - T_{wall,in})}. \tag{11}$$

Here,

$$T_{wall,in} = T_{wall,out} + \Delta T_{wall}, \tag{12}$$

$$\Delta T_{wall} = q_{ref,ts} \times OD \times \frac{\ln(OD/ID)}{(2 \times k_{Cu})}, \tag{13}$$

and also,

$$q_{ref,ts} = \frac{Q_{ref,ts}}{A_{in}}. \tag{14}$$

4. Uncertainty Analysis

The test uncertainty may be computed using Schultz and Cole's equation [36], which is as follows:

$$Ut_R = \left[\sum_{j=1}^{n} \left(\frac{\partial R}{\partial z} Ut_z\right)_j^2\right]^{1/2}. \tag{15}$$

The test uncertainties associated for both estimated and quantitative variables have been documented in Table 4.

5. Findings and Discussion

The data were meticulously examined to explore the impact of many parameters, such as q, G, T_{sat}, and x_{avg}, on the HTC when using R134a refrigerant flowing in smooth and microfin tubes. In addition, a comprehensive assessment analysis was conducted using data collected from multiple tube types to provide a deeper insight into the benefits of enhancing the inner surface of the evaporator. While evaluating the correctness of experimental results, they were compared with multiple flow boiling models proposed by different researchers. The comparisons were carried out to ascertain the durability and consistency of the findings between smooth and microfin tubes.

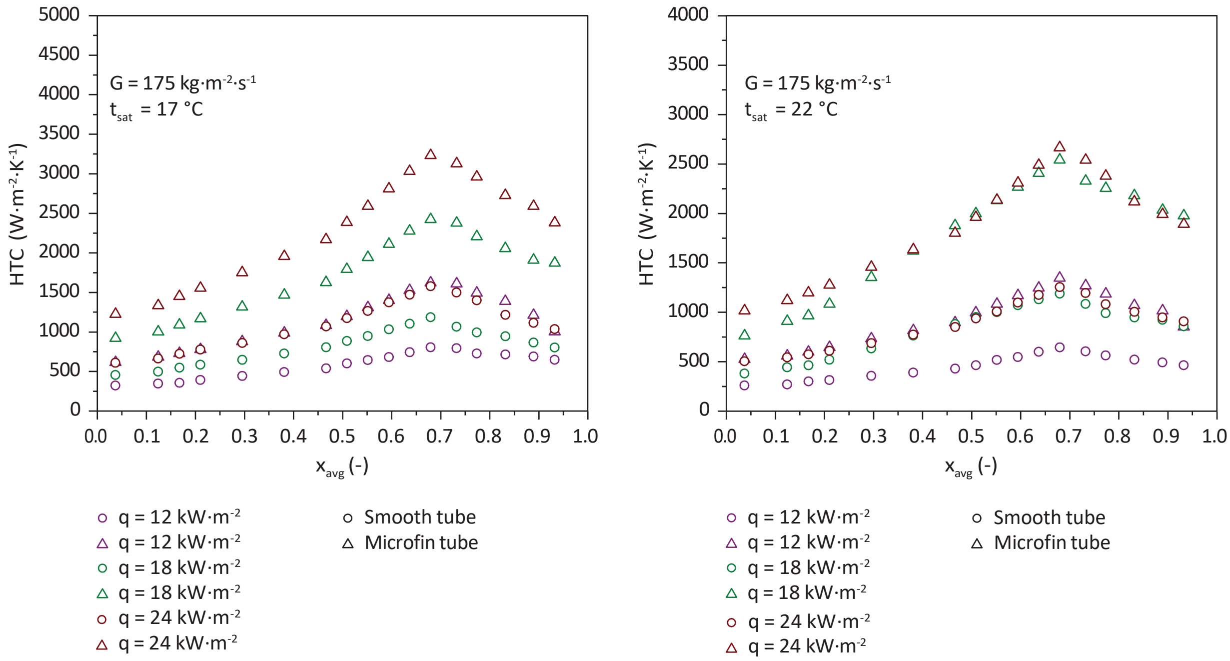

(a) (b)

FIGURE 4: Influence of heat flux on HTC at (a) G � 175 kg.m-2s-1, tsat � 17°C, and (b) G � 175 kg.m-2s-1, tsat � 22°C.

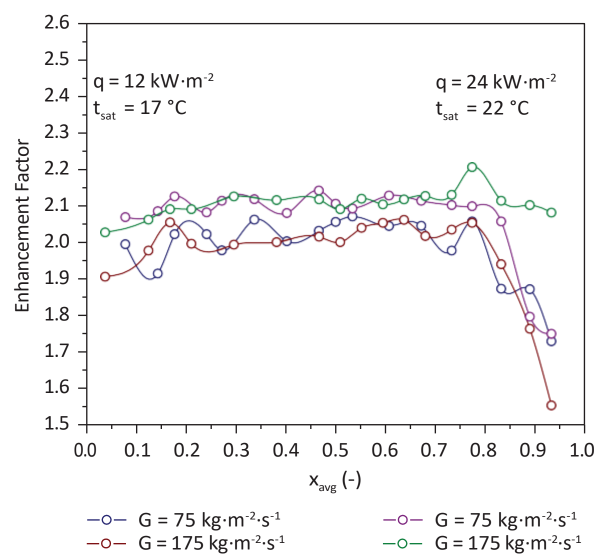

FIGURE 5: Enhancement factor.

5.1. Influence of Mass Flux. An analysis was conducted on the experimental HTC for smooth and micro-fin tubes. This analysis included variable heat flux values of 12, 18 and 24 kW·m^{-2}, three distinct values of G as 75, 125, and 175 kg·m^{-2}·s^{-1}, and T_{sat} values of 290.15 and 295.15 K.

Figure 3 illustrates the influence of mass flux on HTC. HTC with microfin tube outperforms smooth tube in all operating circumstances. In a smooth tube, the influence of mass flux on HTC is considerably greater with low heat flux compared to high heat flux. Furthermore, this influence predominantly manifested within vapor quality's lower to middle range. However, for the smooth, the influence of mass flux on HTC is not consistently present at high T_{sat} circumstances tube. At G � 75 kg·m^{-2}·s^{-1}, q � 12 kWm^{-2}, and T_{sat} � 290.15 K, the microfin tube has 150%–190% higher HTC than smooth tube, whereas at G � 175 kg·m^{-2}·s^{-1}, microfin tube exhibits 165%–270% higher HTC. Similar trends were found in other working circumstances.

As depicted in Figure 3, the HTC for the microfin tube increases as G increases. Range of vapor quality is between 0.02 and 0.93 at q values of 12, 18, and 24 kW·m^{-2}. However,

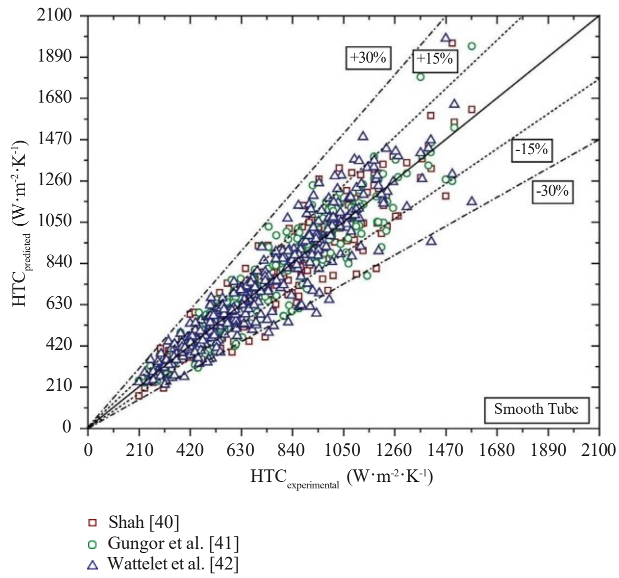

FIGURE 6: Experimental HTC vs. predicted HTC for smooth tubes using FBHT models.

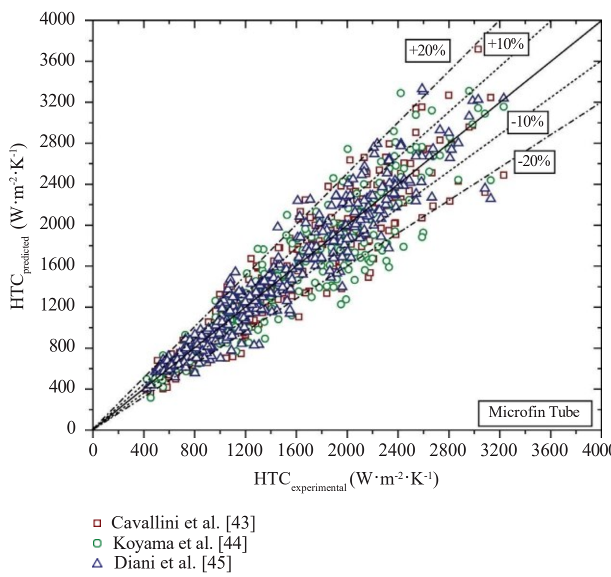

FIGURE 7: Experimental HTC vs. predicted HTC for microfin tubes using FBHT models.

dry-out occurs when the vapor quality reaches a high level (0.725), causing the boiling HTCs' degradation as the G increases. The HTC value at G � 75 kg·m^{-2}·s^{-1} is n significantly different from HTC values at G � 125 kg·m^{-2}·s^{-1} and 175 kg·m^{-2}·s^{-1} within low to midrange of average vapor quality, under all testing conditions. However, when q � 24 kW·m^{-2} and average vapor quality is high, the HTC value is virtually the same for all G values. The dry-out condition occurs beyond the x_{avg} � 0.725, resulting in a heat flux value of 24 kW·m^{-2}. As heat flux enriches, dry-out events for the smooth tube shown in Figures 3(a), 3(b), 3(c), 3(d), 3(e), and 3(f) happen earlier compared to the microfin tube (similar patterns were observed by [29]). A greater q value leads to an enriched inner wall superheat. As a result, the rates at which bubbles expand and separate on the wall increase. The majority of heat transfer during nucleate boiling occurs within intermediate and low x_{avg} zones, exhibiting a strong link between the boiling HTC and the G parameter. Higher values of G reduce the nucleate boiling heat transfer (NBHT) processes by decreasing the number of

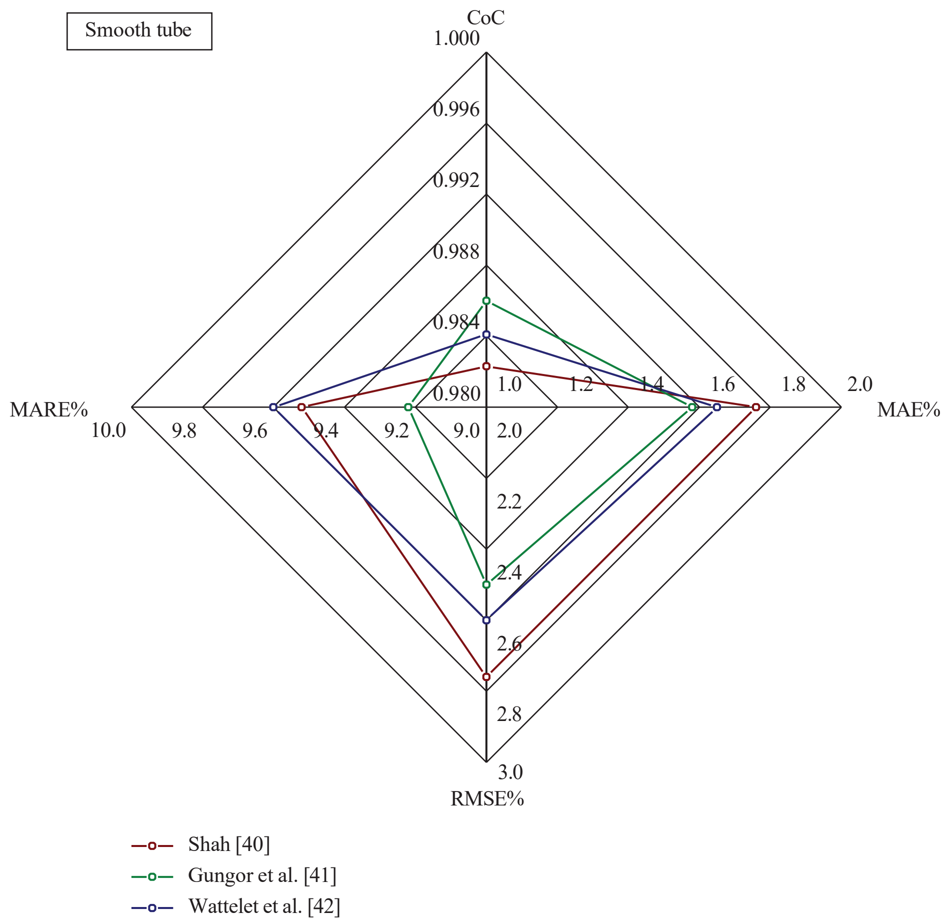

FIGURE 8: Experimental error analysis for the smooth tube utilizing the predicted correlations.

active nucleation sites and preventing inner wall surface from heating [37]. This leads to a greater concentration of vapor and a thinner layer of liquid in the tube, which is beneficial for the NBHToperation. However, in the high x_{avg} zone, forced convection heat transfer is a main factor, and greater G helps to enhance the fluid velocity in the tube.

5.2. Influence of Heat Flux. Major improvements in HTC were encountered at G � 175 kg·m^{-2}·s^{-1}. Impact of heat flux on HTC during distinct working conditions shows similar trends. Hence, it is worth discussing only one condition in detail to understand the impact of heat flux on HTC.

Figure 4 reveals the influence of heat flux on HTC under the following conditions: T_{sat} � 290.15 and 295.15 K and G � 175 kg·m^{-2}·s^{-1}. Microfin tube demonstrates high HTCas comparing with smooth tube. As heat flux in the microfin tube increases, there is tendency for the HTC also to in- crease. Microfins enrich the surface area and create tur- bulence in fluid, improving heat transfer in NBHTprocesses. HTC performance is more noticeable for low volumetric flow rates when NBHT is the main parameter affecting HTC. Combining high heat flux and reduced vapor quality can lead to enriched boiling intensity and improved HTC due to greater vaporization at the tube surface. However, when examining vapor quality values greater than 0.68, it becomes

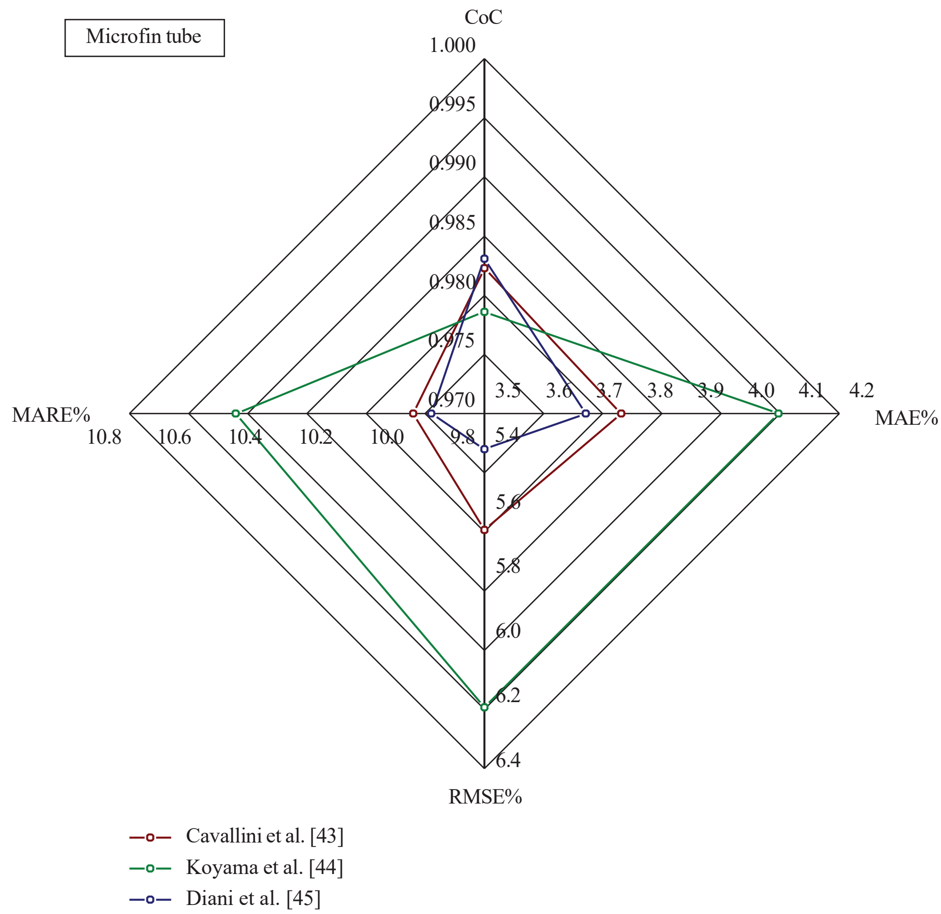

FIGURE 9: Experimental error analysis for the microfin tube utilizing the predicted correlations.

5.3. Comparison with FBHT Models. The experimental HTC results of smooth as well as microfin tubes have been compared to the predicted HTC results calculated from already published FBHT models.

Figure 6 evaluates the HTC predictions for a smooth tube using various models. These models were developed by researchers Shah [40], Gungor and Winterton [41], and Wattelet et al. [42]. The graph reveals that 89% of the experimental data fall in the 15% error range and 96% of the experimental data lie within the 30% error zone. This assessment helps evaluate the reliability of the models and their predictions.

As depicted in Figure 7, the FBHT models developed by Cavallini et al. [43], Koyama et al. [44], and Diani et al. [45] provided valuable insights into HTC predictions for microfin tube. Compared to the predicted data, 82% of experimental HTC are within the error range of 10%. In addition, 92% of experimental HTC are within the 20% error region.

Furthermore, the comparison with recognized FBHT models serves as a compelling validation of their accuracy. As these models are evaluated against experimental data, they demonstrate a high level of precision. These findings endorse the relevance and reliability of these models, making them valuable tools for designing actual HVAC systems. Accurate predictions are crucial for optimizing system performance and ensuring efficient heat transfer in real-world applications.

An error analysis was undertaken to evaluate the precision of the correlation models employed in this study. This analysis included evaluating the following metrics: coefficient of correlation (CoC), mean absolute error (MAE), root mean square error (RMSE), and mean absolute relative error (MARE).

These metrics provide valuable insights into the reliability and precision of the results, endorsing their relevance in actual HVAC system design. The formula for each one can be found as follows:

$$CoC = 1 - \frac{\sum_{j=1}^{N} \left(Z_{j\exp} - Z_{jcal} \right)^2}{\sum_{j=1}^{N} Z_{jcal}^2}, \tag{17}$$

$$MAE = \frac{\sum_{j=1}^{N} \left| Z_{j\exp} - Z_{jcal} \right|}{N}, \tag{18}$$

$$RMSE = \sqrt{\frac{\sum_{j=1}^{N} \left(Z_{j\exp} - Z_{jcal} \right)^2}{N}}, \tag{19}$$

$$MARE = \frac{1}{N} \times \sum_{j=1}^{N} \frac{\left| Z_{j\,cal} - Z_{j\,exp} \right|}{Z_{j\,exp}}. \tag{20}$$

Figure 8 provides the experimental error analysis for the smooth tube. From there, Gungor and Winterton [41] HTC correlation exhibits the lowest error and highest CoC value. Meanwhile, Figure 9 provides the experimental error analysis for micro-fin tube. From there, Diani et al. [45] HTC correlation exhibits the lowest error and highest CoC value.

6. Conclusions

There are several important benefits for microfin tubes when compared to smooth tubes in respect to HTC. Across various test conditions, the microfin tube consistently exhibits superior HTC. Specifically, at a G of 75 kg·m^{-2}·s^{-1}, the microfin tube's HTC is 1.5–1.9 times higher than that of the smooth tube. As mass flux increases to 125 kg m^{-2}·s^{-1} and 175 kg·m^{-2}·s^{-1}, this advantage grows further, reaching 1.6–2.3 times and 1.65 to 2.7 times, respectively.

In addition, at higher heat flux (q = 24 kW·m^{-2}), the microfin tube's HTC significantly improves, being 3.1–5 times higher than at q = 12 kW·m^{-2}. Furthermore, the enhancement factor increases with vapor quality (x_{avg}), particularly for x_{avg} values lower than 0.90.

A number of variables, including as the number of vapor cores, the superheat of the interior wall, and the tube surface properties, affect the occurrence of dry-out. Heat transfer deterioration can occur when heat flux is used to increase heat transfer in the tube, but it can also cause the fluid to violently evaporate and alter the flow pattern.

To assess the HTC results from the current study, a comparison was conducted. Established correlations and models were used for this evaluation. Notably, models de- veloped by Gungor and Winterton [41] for smooth tubes and Diani et al. [45] for microfin tubes demonstrated great accuracy and the lowest error in predicting experimental results.

Nomenclature

A: Area (m^2)
b: Fin root length (mm)
c: Fin tip distance (mm)
$C_{p,l}$: Liquid specific heat (kJ·kg^{-1}·K^{-1})
D: Diameter (mm)
d: Fin root distance (mm)
e: Fin height (mm)
G: Mass flux (kg·m^{-2}·s^{-1})
h: Heat transfer coefficient (kW·m^{-2}·K^{-1})
i_{lv}: Latent heat of evaporation (kJ·kg^{-1})
i: Enthalpy (kJ·kg^{-1})
k_l: Thermal conductivity (kW·m^{-1}·K^{-1})
L: Length of the tube (m)
m: Mass flow rate (kg·s^{-1})
M: Molecular weight (kg·kmol^{-1})
N_{fin}: Number of fins
P: Pressure (kPa)
q: Heat flux (kW·m^{-2})
Q: Heat transfer rate (kW)
S: Perimeter of one fin (mm)
t: Tube thickness (mm)
T: Temperature (K)
t_{wall}: Wall thickness (mm)
w: Fin tip length (mm)
x: Vapor quality
Z: Sample data
HTC: Heat transfer coefficient (W/mm^{-1}K^{-1})
HVAC: Heating, ventilation, and air conditioning
CO_2: Carbon dioxide
CH_4: Methane
CFC: Chlorofluorocarbon
HCFC: Hydrochlorofluorocarbon
ODP: Ozone depletion potential
GWP: Global warming potential
OD: Outer diameter (mm)
ID: Inner diameter (mm)
P_{sat}: Saturation pressure (Pa)
NBHT: Nucleate boiling heat transfer
EF: Enhancement factor (%)
MAE: Mean absolute error (%)
RMSE: Root mean square error (%)
MARE: Mean absolute relative error (%)
CoC: Coefficient of correlation

Greek Letters

α: Apex angle (°)
σ: Surface tension (mN·m^{-1})
ρ: Density (kg·m^{-3})
μ: Dynamic viscosity (μPa·s^{-1})
β: Helix angle (°)

Subscripts

c: Cross-sectional
cal: Calculated
out: Outside
in: Inside
crit: Critical
ref: Refrigerant
ph: Preheater
w: Water
sens: Sensible
ts: Test section
tp: Two-phase
v: Vapor
s: Surface
sat: Saturation
avg: Average
l: Liquid
exp: Experimental.

Data Availability

The data used to support the findings of this study are included within the article.

References

[1] D. J. Wuebbles and J. M. Calm, “An environmental rationale for retention of endangered chemicals,” *Science*, vol. 278, no. 5340, pp. 1090-1091, 1997.

[2] D. Wu, B. Hu, and R. Z. Wang, “Vapor compression heat pumps with pure Low-GWP refrigerants,” *Renewable and Sustainable Energy Reviews*, vol. 138, Article ID 110571, 2021.

[3] C. Yang, S. Seo, N. Takata, K. Thu, and T. Miyazaki, “The life cycle climate performance evaluation of low-GWP refrigerants for domestic heat pumps,” *International Journal of Refrigeration*, vol. 121, pp. 33–42, 2021.

[4] M. O. McLinden, C. J. Seeton, A. Pearson, and A. Pearson, “New refrigerants and system configurations for vapor-compression refrigeration,” *Science*, vol. 370, no. 6518, pp. 791–796, 2020.

[5] J. M. Mendoza-Miranda, C. Salazar-Hern’andez, R. Carrera-Cerritos et al., “Variable speed liquid chiller drop-in modeling for predicting energy performance of R1234yf as low-GWP refrigerant,” *International Journal of Refrigeration*, vol. 93, pp. 144–158, 2018.

[6] N. K. Vidhyarthi, S. Deb, S. S. Gajghate et al., “A comprehensive assessment of two-phase flow boiling heat transfer in micro-fin tubes using pure and blended eco-friendly refrigerants,” *Energies*, vol. 16, no. 4, p. 1951, 2023.

[7] S. Wellsandt and L. Vamling, “Evaporation of R407C and R410A in a horizontal herringbone micro-fin tube: heat transfer and pressure drop,” *International Journal of Refrigeration*, vol. 28, no. 6, pp. 901–911, 2005.

[8] E. P. Bandarra Filho and P. E. L. Barbieri, “Flow boiling performance in horizontal micro finned copper tubes with the same geometric characteristics,” *Experimental Thermal and Fluid Science*, vol. 35, no. 5, pp. 832–840, 2011.

[9] A. Celen and A. S. Dalkılıç, “A complete evaluation method for the experimental data of flow boiling in smooth tubes,” *International Communications in Heat and Mass Transfer*, vol. 89, pp. 108–121, 2017.

[10] M. H. Kim and J. S. Shin, “Evaporating heat transfer of R22 and R410A in horizontal smooth and micro-fin tubes,” *International Journal of Refrigeration*, vol. 28, no. 6, pp. 940–948, 2005.

[11] S. Deb, M. Das, D. C. Das, S. Pal, A. Das, and R. Das, “Significance of surface modification on nucleate pool boiling heat transfer characteristics of refrigerant R-141b,” *International Journal of Heat and Mass Transfer*, vol. 170, Article ID 120994, 2021.

[12] S. Mancin, A. Diani, and L. Rossetto, “R134a flow boiling heat transfer and pressure drop inside a 3.4 mm ID micro-fin tube,” *Energy Procedia*, vol. 45, pp. 608–615, 2014.

[13] E. P. Bandarra Filho and J. M. Saiz Jabardo, “Convective boiling performance of refrigerant R-134a in herringbone and micro-fin copper tubes,” *International Journal of Refrigeration*, vol. 29, no. 1, pp. 81–91, 2006.

[14] A. Kumar, D. C. Das, and P. Das, “Parametric variation studies of experimental flow boiling heat transfer phenomena using R407c inside an enhanced tube,” *Heat and Mass Transfer*, vol. 59, no. 8, pp. 1353–1363, 2023.

[15] K. Hambraeus, “Heat transfer coefficient during two-phase flow boiling of HFC-134a,” *International Journal of Refrigeration*, vol. 14, no. 6, pp. 357–362, 1991.

[16] M. A. Kedzierski and M. P. Kaul, Report NISTIR 5144, *Horizontal Nucleate Flow Boiling Heat Transfer Coefcient Measurements and Visual Observations for R12, R134a and R134a/ester Lubricant Mixtures*, NIST, Gaithersburg, MD, USA, 1993.

[17] X. Huo, L. Chen, Y. S. Tian, and T. G. Karayiannis, “Flow boiling and flow regimes in small diameter tubes,” *Applied Thermal Engineering*, vol. 24, no. 8-9, pp. 1225–1239, 2004.

[18] E. P. Bandarra Filho and P. E. Barbieri, “Flow boiling performance in horizontal microfinned copper tubes with the same geometric characteristics,” *Experimental Thermal and Fluid Science*, vol. 35, no. 5, pp. 832–840, 2011.

[19] A. Greco and G. P. Vanoli, “Evaporation of refrigerants in a smooth horizontal tube: prediction of R22 and R507 heat transfer coefficients and pressure drop,” *Applied Thermal Engineering*, vol. 24, no. 14-15, pp. 2189–2206, 2004.

[20] S. Koyama, J. Lee, and R. Yonemoto, “An investigation on void fraction of vapor-liquid two-phase flow for smooth and micro-fin tubes with R134a at adiabatic condition,” *International Journal of Multiphase Flow*, vol. 30, no. 3, pp. 291–310, 2004.

[21] W. Cui, L. Li, M. Xin, T. C. Jen, Q. Liao, and Q. Chen, “An experimental study of flow pattern and pressure drop for flow boiling inside micro-finned helically coiled tube,” *International Journal of Heat and Mass Transfer*, vol. 51, no. 1-2, pp. 169–175, 2008.

[22] V. D. Hatamipour and M. A. Akhavan-Behabadi, “Visual study on flow patterns and heat transfer during convective boiling inside horizontal smooth and micro-fin tubes,” *World Academy of Sceince, Engineering and Technology*, vol. 69, pp. 700–706, 2010.

[23] L. P. Colombo, A. Lucchini, and A. Muzzio, “Flow patterns, heat transfer and pressure drop for evaporation and condensation of R134A in micro-fin tubes,” *International Journal of Refrigeration*, vol. 35, no. 8, pp. 2150–2165, 2012.

[24] G. Bamorovat Abadi, E. Yun, and K. C. Kim, “Flow boiling characteristics of R134a and R245fa mixtures in a vertical circular tube,” *Experimental Thermal and Fluid Science*, vol. 72, pp. 112–124, 2016.

[25] T. Wen, H. Zhan, and D. Zhang, “Flow boiling heat transfer in mini channel with serrated fins: experimental investigation and development of new correlation,” *International Journal of Heat and Mass Transfer*, vol. 128, pp. 1081–1094, 2019.

[26] A. Diani, S. Mancin, and L. Rossetto, “Flow boiling heat transfer of R1234yf inside a 3.4mm ID microfin tube,” *Experimental Thermal and Fluid Science*, vol. 66, pp. 127–136, 2015.

[27] A. Diani and L. Rossetto, “Characteristics of R513A evaporation heat transfer inside small-diameter smooth and micro-fin tubes,” *International Journal of Heat and Mass Transfer*, vol. 162, Article ID 120402, 2020.

[28] A. Diani and L. Rossetto, “Experimental analysis of refrigerants flow boiling inside small-sized micro-fin tubes,” *Heat and Mass Transfer*, vol. 54, no. 8, pp. 2315–2329, 2018.

[29] A. Celen, A. Çebi, and A. S. Dalkılıç, “Investigation of boiling heat transfer characteristics of R134a flowing in smooth and

micro-fin tubes," *International Communications in Heat and Mass Transfer*, vol. 93, pp. 21–33, 2018.

[30] G. Righetti, G. A. Longo, C. Zilio, R. Akasaka, and S. Mancin, "R1233zd(E) flow boiling inside a 4.3mm ID micro-fin tube," *International Journal of Refrigeration*, vol. 91, pp. 69–79, 2018.

[31] S. Deb, P. M. Kanade, S. Pal, and A. K. Das, "Influence of horizontal enhanced tube on flow boiling heat transfer characteristics of environmentally friendly refrigerant R-407c," *Materials Today: Proceedings*, vol. 62, no. 6, pp. 3178–3182, 2022.

[32] S. Deb, K. P. Mahesh, M. Das et al., "Flow boiling heat transfer characteristics over horizontal smooth and micro-fin tubes: an empirical investigation utilizing R407c," *International Journal of Thermal Sciences*, vol. 188, Article ID 108239, 2023.

[33] N. K. Vidhyarthi, S. Deb, S. Pal, and A. K. Das, "Significance of enhanced Cu-tube over flow boiling heat transfer characteristics using R134a: an experimental investigation," *Materials Today: Proceedings*, 2023.

[34] S. Deb, N. K. Vidhyarthi, S. Pal, A. K. Das, and D. Barik, "Parametric evaluation of the flow boiling heat transfer properties of R22 and R407c inside horizontal micro-fin tube," *International Journal of Energy Research*, vol. 2023, Article ID 8882662, 14 pages, 2023.

[35] E. W. Lemmon, M. L. Huber, and M. O. McLinden, *NIST Standard Reference Database 23, NIST Reference Fluid Thermodynamic and Transport Properties, REFPROP, Version 9.0. Standard Reference Data Program*, National Institute of Standards and Technology, Gaithersburg, MD, USA, 2018.

[36] R. R. Schultz and R. Cole, "Uncertainty analysis in boiling nucleation," *AIChE Symposium Series*, vol. 189, pp. 32–38, 1979.

[37] G. He, S. Zhou, D. Li, D. Cai, and S. Zou, "Experimental study on the flow boiling heat transfer characteristics of R32 in horizontal tubes," *International Journal of Heat and Mass Transfer*, vol. 125, pp. 943–958, 2018.

[38] A. Arcasi, A. W. Mauro, G. Napoli, and L. Viscito, "Heat transfer coefficient, pressure drop and dry-out vapor quality of R454C. Flow boiling experiments and assessment of methods," *International Journal of Heat and Mass Transfer*, vol. 188, Article ID 122599, 2022.

[39] A. Padovan, D. Del Col, and L. Rossetto, "Experimental study on flow boiling of R134a and R410A in a horizontal micro-fin tube at high saturation temperatures," *Applied Thermal Engineering*, vol. 31, no. 17-18, pp. 3814–3826, 2011.

[40] M. M. Shah, "Chart correlation for saturated boiling heat transfer: equations and further study," *ASHRAE Transactions*, vol. 88, pp. 185–196, 1982.

[41] K. E. Gungor and R. H. S. Winterton, "Simplified general correlation for saturated flow boiling and comparison with data," *Chemical Engineering Research and Design*, vol. 65, pp. 148–156, 1987.

[42] J. P. Wattelet, J. C. Chato, A. L. Souza, and B. R. Christoffersen, "Evaporative characteristics of R-12, R-134a, and a mixture at low mass fluxes," *ASHRAE Transactions*, vol. 94, pp. 603–615, 1994.

[43] A. Cavallini, D. Del Col, L. Doretti, G. A. Longo, and L. Rossetto, "Refrigerant vaporization inside enhanced tubes: a heat transfer model," *Heat and Technology*, vol. 17, no. 1, pp. 29–36, 1999.

[44] S. Koyama, J. Yu, S. Momoki, T. Fujii, and H. Honda, "Forced convective flow boiling heat transfer of pure refrigerants inside a horizontal micro-fin tube," in *Proceedings of the Convective Row Boiling Conference*, pp. 137–142, Taylor and Francis, Banff, Canada, May 1995.

[45] A. Diani, S. Mancin, and L. Rossetto, "R1234ze(E) flow boiling inside a 3.4 mm ID micro-fin tube," *International Journal of Refrigeration*, vol. 47, pp. 105–119, 2014.